COMMUNICATION

A Face-to-Face Orchestration of Quasiplanar Donor and Acceptor Enables Highly Efficient Intramolecular Exciplex Fluorescence

Chao Wu,[a] Weiqiang Liu,[b] Kai Li,*[a] Gang Cheng,*[b] Jinfan Xiong,[a] Teng Teng,[a] Chi-Ming Che,[b] and Chuluo Yang*[a]

[a] C. Wu, Dr. K. Li, J. Xiong, Dr. T. Teng, Prof. Dr. C. Yang
College of Materials Science and Engineering, Shenzhen University
Shenzhen 518055 (P. R. China)
E-mail: kaili@szu.edu.cn; clyang@szu.edu.cn
[b] W. Liu, Dr. G. Cheng, Prof. Dr. C.-M. Che
State Key Laboratory of Synthetic Chemistry, HKU-CAS Joint Laboratory on New Materials, and Department of Chemistry
The University of Hong Kong
Pokfulam Road, Hong Kong (P. R. China)
E-mail: ggcheng@hku.hk

Supporting information for this article is given via a link at the end of the document.

Abstract: Intramolecular through-space charge-transfer (TSCT) excited state has been exploited for developing thermally activated delayed fluorescence (TADF) emitters, whereas the tuning of excited state dynamics via conformational engineering remains sparse. Herein we designed a series of TSCT emitters with precisely controlled alignment of the donor and acceptor segments. With increasing intramolecular π-π interactions, the radiative decay rate of the lowest singlet excited state (S_1) progressively increased together with a suppression of nonradiative decay, leading to significantly enhanced photoluminescence quantum yields up to 0.99 in doped thin films. High-efficiency electroluminescence device with maximum external quantum efficiency (EQE) of 23.96% has been achieved which maintains at >20% at the brightness of 1000 cd m^{-2}. This work sheds light on the importance of conformation control for achieving high-efficiency intramolecular exciplex emitters.

Pure organic emitters radiating via thermally-activated delayed fluorescence (TADF) promise high-efficiency organic light-emitting diodes (OLEDs) without resorting to noble metal elements in harvesting triplet excitons.[1] It remains a challenge to design TADF molecules having both high photoluminescence quantum yield (PLQY) and short delayed emission lifetime because of the inherent conflict between a strong oscillator strength for the lowest singlet excited state (S_1) radiation and a fast reverse intersystem crossing (RISC) from the lowest triplet excited state (T_1) to S_1 which impose opposite requirements on the frontier molecular orbitals overlap integral.[2]

Intramolecular exciplex has emerged as an appealing TADF candidate owing to its intrinsic small energy difference between the singlet and triplet excited states (ΔE_{ST}) of through-space charge transfer (TSCT) nature.[3-6] Obviously, the distance and orientation between the donor and acceptor segments are crucial to the excited state dynamics of an intramolecular exciplex. As depicted in Figure 1a-c, edge-to-face and slipped face-to-face alignments have been usually encountered in the design of TSCT emitters.[3,4b,7] Without taking into account the precise orientation of the π-orbitals of the donor and acceptor, only weak interactions between non-hydrogen atoms or the best-fit planes are present. Recently, advances of manipulating the cofacial π-π interaction have been made through elegant choice or design of molecular scaffolds to accommodate the donor and acceptor (Figure 1d).[8,9] Thanks to these conformational engineering, the photo- and electroluminescence efficiencies have been remarkably enhanced due to the suppressed nonradiative decay and/or accelerated RISC. Nevertheless, the tuning of radiative decay has not been unveiled and the distance between donor and acceptor in these molecules is still too longer for effective face-to-face π-π interaction to occur. We envision that cofacial arrangement of the donor and acceptor should have a positive influence on the intramolecular exciplex formation and its radiative transition.[10]

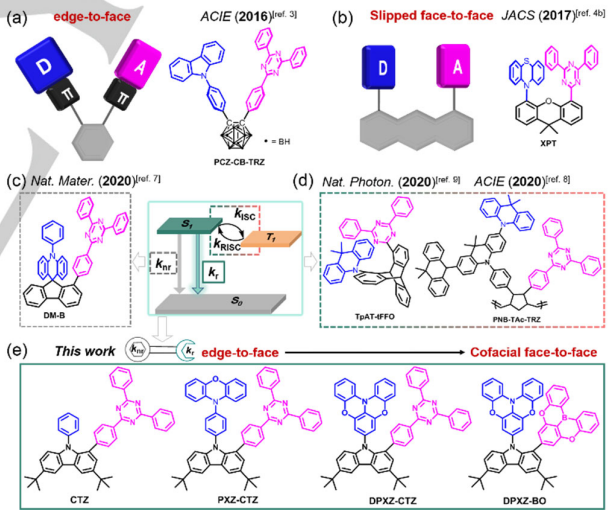

Figure 1. (a-b) Representative molecular architectures for the design of TSCT emitters. TSCT TADF emitters featuring (c-d) suppressed nonradiative decay, or facilitated reverse intersystem crossing. (e) Chemical structures of the emitters in this study featuring controlled donor-acceptor orientations.

Herein, we report an orchestration of donor and acceptor in carbozole-bridged intramolecular exciplex TADF emitters (Figure 1e) with controlled orientations from orthogonal to cofacial. The PLQY has been increased from 0.5 to 0.99 because of the significantly increased radiative decay rate and suppressed nonradiative decay. The optimized emitter has demonstrated a maximum EQE of 24% and a small efficiency roll-off for OLEDs. A very small efficiency roll-off down to 1% at 1000 cd m^{-2} was also

revealed for devices using this type of emitter when a co-host was used.

Phenoxazine (PXZ) and triphenyltriazine (TRZ) were first selected as the donor and the acceptor to design **PXZ-CTZ** in which the geometric restraint would force the PXZ to be orthogonal to TRZ. In **DPXZ-CTZ**, the three aryl groups on N atom were fused into a quasiplane (DPXZ) which can parallel TRZ.[11] Further, **DPXZ-BO** was designed by replacing TRZ with a rigid O-bridged triphenylborane (BO) which has an ideal matching shape with the DPXZ donor and may invoke charge transfer within the B-N frustrated Lewis pair.[12] A control compound **CTZ** was designed for comparative study. Their syntheses are provided in the Supporting Information. The acceptor and donor were introduced to the 3,6-di-*tert*-butylcarbazole through Suzuki and Buchwald cross-coupling reactions in high yields. All molecules were characterized by various spectroscopic methods (multinuclear NMR, high-resolution mass spectrometry) and single-crystal X-ray diffraction analysis (see crystal data in Table S1, Supporting Information). As shown in Figure 2a, the precise control over donor-acceptor orientations are manifested by their X-ray crystal structures. The TRZ planes are tilted by 48-56° from the carbazole bridge in **CTZ**, **PXZ-CTZ**, and **DPXZ-CTZ** (Figure S1, Supporting Information). A dihedral angle of ca. 84° between the phenoxazine (PXZ) plane (defined by N1-C7-C9) and the TRZ plane was determined in **PXZ-CTZ**, revealing an edge-to-face alignment. The close contacts were found for C65-N37 and C16-C33 with distances of 3.415 and 3.142 Å, respectively (Figure 2b, top). In contrast, the crystal structure of **DPXZ-CTZ** reveals favoured π-π interactions within the donor-acceptor pair. Except that the DPXZ segment is a little ruffled, one Ph ring of it closely stacks with the central triazine ring with π-π distances of 3.3-3.6 Å (Figure 2b, middle). The closest distance between C atoms of the donor and acceptor is 2.982 Å (C8-C30). The N1-N5 distance of 3.759 Å signifies the involvement of lone electron pair of N1 in the interactions. In **DPXZ-BO**, both the donor and acceptor twist to a slightly larger degree with respect to the carbazolyl bridge. Specially, the deformation of the acceptor from an ideal planar structure is similar to that of DPXZ. These two structural features lead to a close cofacial π-π stacking of 3.2-3.6 Å involving most of the atoms of the two quasiplanes (Figure 2b, bottom). An angle of ca. 30° between N1-B bond and the normal of the acceptor plane (Figure S1) also reveals the substantial overlap of their π-electron clouds. The increased π-π stacking from **PXZ-CTZ** to **DPXZ-BO** can also be viewed from their space-filling structures (Figure 2c). Reduced density gradient (RDG) analysis of their crystal structures verified the enhancement in non-covalent van der Waals interactions from **PXZ-CTZ** to **DPXZ-BO** (Figure 2d-e).

DFT and TDDFT calculations were first performed on **PXZ-CTZ**, **DPXZ-CTZ**, and **DPXZ-BO** to study their electronic structures on the basis of crystal structures. As expected, the HOMO and LUMO for each molecule in ground state (S_0) majorly localize on the donor and the acceptor segments (Figure 2f-g). The weak oscillator strength (*f*) of 5×10^{-4}-1.2×10^{-3} for S_0-S_1 transitions and the small calculated ΔE_{ST} values of 0.003-0.028 eV are characteristics of charge-transfer transition (Figure S2, Supporting Information). For comparison, ground state geometries were also optimized by DFT and used for the analyses (Figure S3, Supporting Information). The donor and acceptor in **PXZ-CTZ** are found to be parallel to each other and the donor-acceptor distances in **DPXZ-CTZ** and **DPXZ-BO** are shorter than those determined by X-ray diffraction, probably due to the overestimation of π-π interactions in the calculations. While, the trend in increasing π-π interactions from **PXZ-CTZ** to **DPXZ-BO** is reproduced. Pronounced charge-transfer character for the excited states were also characterized with similar frontier molecular orbitals distributions. Therefore, the excited state analyses based on crystal structures and DFT-optimized geometries both suggest their favourable TADF emission.

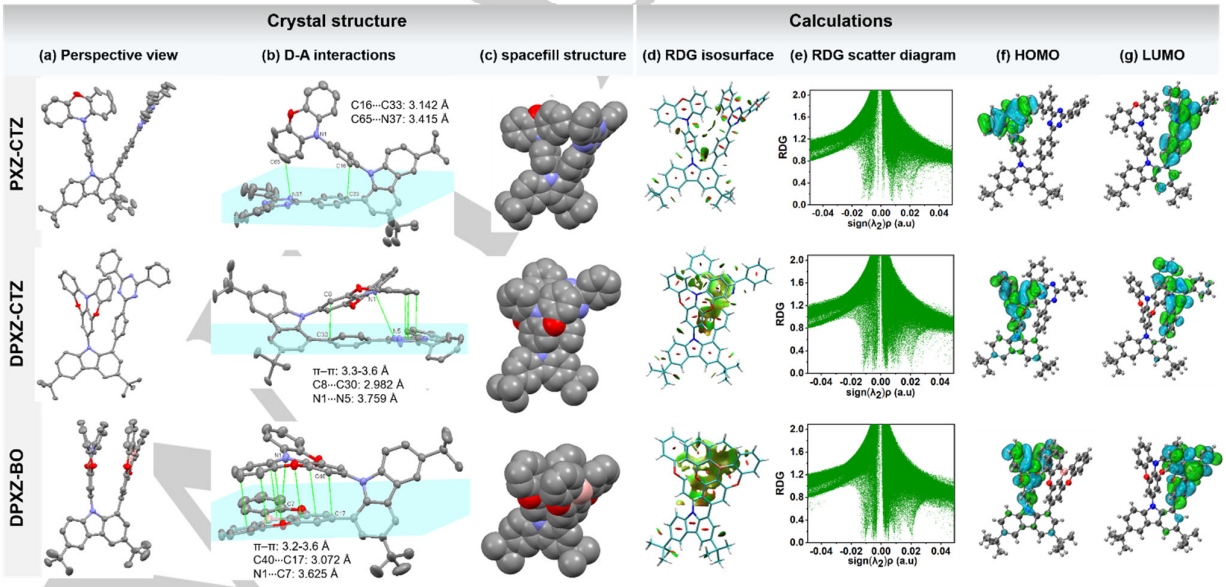

Figure 2. (a) Perspective view of the single-crystal structures, (b) illustration of the intramolecular interactions, and (c) spacefill structures of **PXZ-CTZ**, **DPXZ-CTZ**, and **DPXZ-BO**. (d) Calculated reduced density gradient (RDG) isosurfaces and (e) scattering diagrams on the basis of single crystal structures. (f) HOMO and (g) LUMO plots from the DFT calculations of the crystal structures.

All of the four molecules exhibit broad structureless absorption in the region of 360-400 nm (Figure 3a). With reference to previous report, they are assigned to charge-transfer transitions from carbazole bridge to the TRZ or BO acceptor.[13] Comparing to **CTZ**, the evidently increased molar absorptivity of **PXZ-CTZ**, **DPXZ-CTZ**, and **DPXZ-BO** in this region stems from the absorptions of the donors. Notably, the electronic transitions from the spatially separated donor to the acceptor via through-space charge-transfer are not observed for **PXZ-CTZ**, **DPXZ-CTZ**, and **DPXZ-BO**, implying the absence of effective electronic coupling within the intramolecular donor-acceptor pair.[9,14] The torsional dynamics of the donors and acceptors in fluid solution are conceived to loosen the intramolecular π-π contact in ground state.

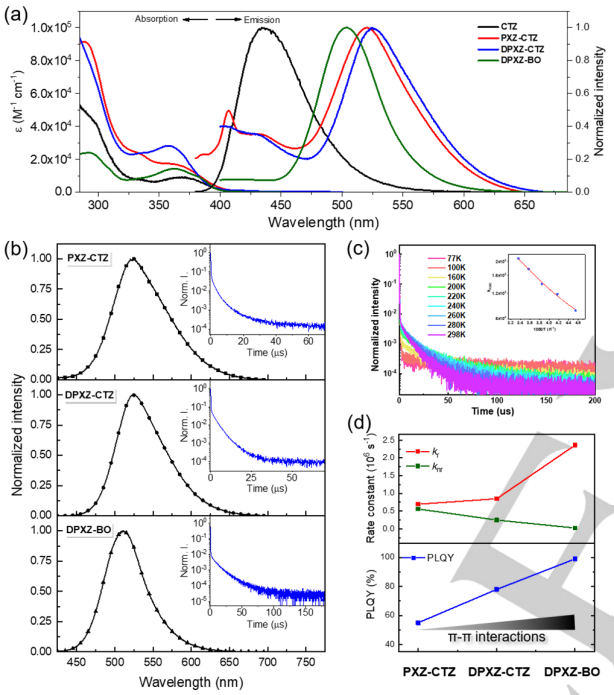

Figure 3. (a) UV-Vis absorption and emission spectra of **CTZ**, **PXZ-CTZ**, **DPXZ-CTZ** and **DPXZ-BO** in toluene (1×10^{-5} M) at 298 K. (b) Steady-state photoluminescence spectra and the transient PL decay characteristic of **PXZ-CTZ**, **DPXZ-CTZ** and **DPXZ-BO** in DPEPO at 298 K. (c) Variable temperature transient PL decay characteristics of **DPXZ-BO** in DPEPO at 77-298 K; inset: Arrhenius analysis of the k_{RISC} versus temperature (220-300 K). (d) Plot of PLQY, k_r and k_{nr} *versus* the strength of π-π interactions.

In toluene at room temperature, all of the four compounds exhibit structureless emissions while additional weak, structured emission bands are observed for **PXZ-CTZ** and **DPXZ-CTZ** which are tentatively assigned as local excitation (LE) states of the donor or acceptor fragment (Figure 3a). The co-existence of multiple bright states is reminiscent of the photophysical properties for triad molecules comprising multiple donors and/or acceptors.[3,5c,10a] Unlike their comparable energies for the charge-transfer absorption, the dominant emission spectra of **PXZ-CTZ**, **DPXZ-CTZ**, and **DPXZ-BO** are significantly redshifted by 69-91 nm from that of **CTZ**. Comparison of the absorption and emission spectra of **CTZ** reveals the same parentage (carbazole→TRZ) for both of its $S_0\rightarrow S_1$ and $T_1\rightarrow S_0$ transitions. The lower-energy emissions for **PXZ-CTZ**, **DPXZ-CTZ**, and **DPXZ-BO** are assigned to come from an intramolecular exciplex. All exciplex emitters **PXZ-CTZ**, **DPXZ-CTZ**, and **DPXZ-BO** display intense and single emissions in doped (diphenylphosphino)phenyl]ether oxide (DPEPO) films at room temperature (Figure 3b), suggestive of favoured donor-acceptor association in solid state. Transient PL studies clearly showed the presence of long-lived emission (Figure 3b), which can be assigned to TADF on the basis of variable temperature photoluminescence decay characteristics (Figure 3c and Figure S4). The lifetimes for prompt and delayed fluorescence (PF and DF) were determined to be 117-183 ns and 3.38-11.3 μs (Table 1). Time-resolved photoluminescence spectra at 77 K reveal small ΔE_{ST} values less than 0.07 eV (Figure S5), accounting for their favoured TADF properties. An Arrhenius analyses of the temperature-dependent k_{RISC} of **DPXZ-BO** gives an activation energy of 0.09 eV (Figure 3c), likely suggesting the presence of an upper-lying intermediating state for the RISC process. Remarkably, the PLQY is increased from 0.55 for **PXZ-CTZ** to 0.78 for **DPXZ-CTZ**, and to 0.99 for **DPXZ-BO** with the DF portions estimated to be 0.58-0.87 (Table 1). Kinetic analysis reveals progressive increase in the radiative decay rates of the S_1 state ($k_{r,S}$) with increasing π-π interactions. On the other hand, the intramolecular motion of both the donor and the acceptor in a strongly bound exciplex is conceived to be restricted, leading to supressed nonradiative decay. Both factors render **DPXZ-BO** having the highest PLQY. Of note, **DPXZ-CTZ** has the largest k_{ISC} and k_{RISC} values which is likely due to its almost energetic degenerate S_1 and T_1 states and/or favoured mediation effect of close-lying triplet excited states. The emission properties of the emitters in 1,3-bis(N-carbazolyl)benzene (mCP) and in neat films were also examined (Figure S6 and Table S2, Supporting Information). The shorter emission lifetimes for neat film are likely due to the concentration quenching effect. In contrast, **CTZ** was found to possess a large ΔE_{ST} of ca. 0.5 eV, interpreting its sole prompt fluorescence.

Table 1. Physical data of **PXZ-CTZ**, **DPXZ-CTZ**, and **DPXZ-BO** in DPEPO films

Compound	λ_{em} (nm)[a]	Φ[a]	ΔE_{ST} (eV)[b]	τ_{PF} (ns)/τ_{DF} (μs)	η_{DF}[c]	$k_{r,S}$ (s^{-1})[d]	$k_{nr,S}$ (s^{-1})[d]	k_{ISC} (s^{-1})[e]	k_{RISC} (s^{-1})[e]
PXZ-CTZ	525	0.55	0.07	183/3.41	0.77	6.95×10^5	5.62×10^5	4.21×10^6	1.28×10^6
DPXZ-CTZ	524	0.78	-0.03	117/3.38	0.87	8.48×10^5	2.46×10^5	7.45×10^6	2.31×10^6
DPXZ-BO	511	0.99	0.03	178/11.3	0.58	2.36×10^6	2.38×10^4	3.24×10^6	2.10×10^5

[a] With emitter concentration of 20 wt% and measured under argon atmosphere. [b] Excited state energy estimated from the onset of fluorescence and phosphorescence spectra at 77 K. [c] Ratio of TADF in the total fluorescence. [d] Radiative and nonradiative decay rates of S_1 state. [e] Intersystem crossing (ISC) and reverse intersystem crossing (RISC) rates between S_1 and T_1 states.

In the context of conformational engineering towards efficient TSCT emitters, an effective suppression of nonradiative decay has recently been realized by spatially confining the donor and acceptor.[7] On the other hand, the manipulation of π-π interaction has been demonstrated to be useful for boosting the RISC rate through tuning the relative energy levels of ^{1}CT, ^{3}CT and ^{3}LE states.[9] While, effect of π-π interactions on the radiative decay rate (k_r) of S_1 state has not been elucidated although it plays a crucial role in governing the total PLQY. Figure 3d illustrates the dependence of k_r, k_{nr} and PLQY on the π-π interactions. It can be seen that simultaneous increase in k_r and decrease in k_{nr} are resulted with increasing π-π interaction. Intermolecular exciplex emitter via co-crystal engineering has also been explored for TADF but only displayed a low PLQY.[15] In spite of the presence of multiple intermolecular non-covalent interactions, conformation and orientation control towards co-facial π-π stacking has not been achieved. The findings in the present work implies that the alignment of structurally similar donor and acceptor segments could maximize π-π interactions to further improve the emission properties of intermolecular charge transfer complexes.

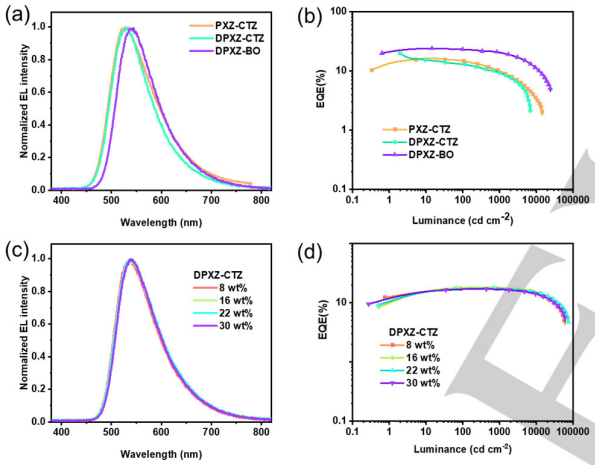

Figure 4. (a) Normalized EL spectra and (b) EQE *versus* luminance of devices using DPEPO as the host. (c) Normalized EL spectra and (d) EQE *versus* luminance of devices with various concentrations of **DPXZ-CTZ** doped into TCTA:B3PYMPM.

The excellent thermal stability with T_d of 408-425° (Figure S7, Supporting Information) and high-yields sublimation (>90%) of **PXZ-CTZ**, **DPXZ-CTZ**, and **DPXZ-BO** are highly beneficial for OLEDs fabrication by vacuum deposition. With their FMO energy levels estimated by electrochemical measurements (Figure S8 and Table S3, Supporting Information), OLEDs with a device structure of ITO/HAT-CN (5 nm)/TAPC (40 nm)/TCTA (8 nm)/mCP (8 nm)/DPEPO:emitter (20 nm)/DPEPO (10 nm)/TmPyPB (40 nm)/LiF (1 nm)/Al (100 nm) were fabricated by vacuum-deposition to evaluate the potential application of **PXZ-CTZ**, **DPXZ-CTZ**, and **DPXZ-BO**. The chemical structures and FMO energy levels of 1,4,5,8,9,11-hexaazatriphenylene hexacarbonitrile (HAT-CN), di-[4-(*N*,*N*-ditolyl-amino)-phenyl]cyclohexane (TAPC), 4,4',4"-tris(carbazole-9-yl)triphenylamine (TCTA), DPEPO, and 1,3,5-tris[(3-pyridyl)phen-3-yl]benzene (TmPyPB) are depicted in Figures S9 and S10 (Supporting Information). HAT-CN, TAPC, TmPyPB serve as hole-injection, hole-transporting, and electron-transporting layers, respectively. The bilayer TCTA/mCP was inserted between the emission layer (EML) and the hole-transporting layer to confine excitons and electrons inside the EML as well as to facilitate the hole-injection to EML. Likewise, a thin layer of DPEPO (10 nm) was inserted for exciton/hole-blocking. Detailed device data are provided in Figures S11-S13 and Tables S4-S6 (Supporting Information). As shown in Figure 4a, the optimized devices exhibit electroluminescence (EL) with Commission International de l'Eclairage (CIE) coordinates of (0.33, 0.56), (0.39, 0.57), and (0.26, 0.58) for **PXZ-CTZ**, **DPXZ-CTZ** and **DPXZ-BO**, respectively. The maximum EQE/current efficiency/power efficiency are 23.96%/76.74 cd A^{-1}/65.63 lm W^{-1} for the device with 30 wt% **DPXZ-BO**. In consistence with their PLQYs, relatively lower maximum EQEs of 19.71% and 16.57% were obtained for the **DPXZ-CTZ**- and **PXZ-CTZ**-based devices (Figure 4b). Remarkably, the maximum efficiencies of the **DPXZ-BO**-based devices are insensitive to the dopant concentration in the tested range of 8%-40% (Figure S13 and Table S6, Supporting Information). This feature is highly beneficial for OLED fabrication where the precise control of dopant concentrations is no more essential.[3,14,16] Interestingly, the devices showed reduced efficiency roll-off at high brightness when dopant concentration is increased. For example, the roll-off of EQEs at 1000 cd m^{-2} for **DPXZ-BO** at 12%, 20%, 30% and 40% doping levels are 37.2%, 24.1%, 15.6% and 11.5%, respectively. As a result, the EQE remains >20% for 30 wt.% **DPXZ-BO** doped device at the luminance level of 1000 cd m^{-2}. Similar features were also observed for **PXZ-CTZ** and **DPXZ-CTZ** based devices.

The potential of these emitters were also examined by using a co-host strategy in a device structure of ITO/HAT-CN (5 nm)/TAPC (40 nm)/TCTA (10 nm)/TCTA:B3PYMPM:Emitter (20 nm)/B3PYMPM (10 nm)/TmPyPB (40 nm)/LiF (1 nm)/Al (100 nm) where 4,6-Bis(3,5-di(pyridin-3-yl)phenyl)-2-MethylpyriMidine (B3PYMPM) is used as electron-transporting material and its structure as well FMO energy levels shown in Figures S9 and S10 (Supporting Information). The device data are provided in Figures S14-S16 and Tables S7-S9 (Supporting Information). **DPXZ-CTZ** offered superior performances than **DPXZ-BO**. First, the EL spectra are stable against the variations of dopant concentration of 8-30 wt% (Figure 4c). The maximum brightness of 75100 cd m^{-2} is remarkably high among the TSCT emitters in the literature. Although the maximum EQE of 17.95% is comparable to that in DPEPO host, its roll-off was found to be as small as only 1.1% at 1000 cd m^{-2} (Figure 4d), which is among the best values for OLEDs regardless of the emission mechanism.[8] Even at the brightness of 10000 cd m^{-2}, the EQE remains >15%. The high maximum luminance, EQE, and exceptionally low efficiency roll-off collectively promise this type of molecules as robust OLED emitters provided a suitable host was identified.

In summary, a new class of intramolecular exciplex TADF emitters featuring TSCT excited states have been developed and demonstrated appealing performances in OLEDs. The control over alignment of donor and acceptor towards strong cofacial π-π interaction has been validated to be effective in enhancing the PLQYs. A positive correlation between radiative rates and the strength of π-π interaction has been revealed. The tuning of the radiative decay of singlet excited state by conformation and orientation engineering presents an important step forward in the

design of TSCT TADF emitters. By referring to the strategy for boosting RISC via ^{3}LE state mediation in the design of through-bond charge transfer TADF emitters, TSCT emitters possessing simultaneous high emission efficiency and short-lived delayed emission are highly expected.

Acknowledgements

This work was supported by National Natural Science Foundation of China (21801170 and 91833304 and), the Shenzhen Science and Technology Program (KQTD20170330110107046), the Science and Technology Innovation Commission of Shenzhen Municipality (JCYJ20190808172203553). K.L. acknowledges the support from the Department of Science and Technology of Guangdong Province (2019QN01C617).

Keywords: OLED • TADF • Exciplex • Through-Space Charge Transfer • Orientation Control

[1] H. Uoyama, K. Goushi, K. Shizu, H. Nomura, C. Adachi, *Nature* **2012**, *492*, 234-238.

[2] a) Q. Zhang, H. Kuwabara, W. J. Potscavage, S. Huang, Y. Hatae, T. Shibata, C. Adachi, *J. Am. Chem. Soc.* **2014**, *136*, 18070-18081; b) K. Shizu, M. Uejima, H. Nomura, T. Sato, K. Tanaka, H. Kaji, C. Adachi, *Phys. Rev. Appl.* **2015**, *3*, 014001; c) S. Hirata, Y. Sakai, K. Masui, H. Tanaka, S. Y. Lee, H. Nomura, N. Nakamura, M. Yasumatsu, H. Nakanotani, Q. Zhang, K. Shizu, H. Miyazaki, C. Adachi, *Nat. Mater.* **2015**, *14*, 330-336; d) Q. Ai, J. Chai, W. Lou, T. Liu, D. Wang, C. Deng, C. Wang, G. Li, X. Liu, Z. Liu, Q. Zhang, *ACS Appl. Mater. Interfaces* **2020**, *12*, 6127-6136.

[3] R. Furue, T. Nishimoto, I. S. Park, J. Lee, T. Yasuda, *Angew. Chem. Int. Ed.* **2016**, *55*, 7171-7175; *Angew. Chem.* **2016**, *128*, 7287-7291.

[4] a) K. Kawasumi, T. Wu, T. Zhu, H. S. Chae, T. Van Voorhis, M. A. Baldo, T. M. Swager, *J. Am. Chem. Soc.* **2015**, *137*, 11908-11911; b) H. Tsujimoto, D.-G. Ha, G. Markopoulos, H. S. Chae, M. A. Baldo, T. M. Swager, *J. Am. Chem. Soc.* **2017**, *139*, 4894-4900.

[5] a) Y. H. Lee, S. Park, J. Oh, J. W. Shin, J. Jung, S. Yoo, M. H. Lee, *ACS Appl. Mater. Interfaces* **2017**, *9*, 24035-24042; b) E. Spuling, N. Sharma, I. D. W. Samuel, E. Zysman-Colman, S. Bräse, *Chem. Commun.* **2018**, *54*, 9278-9281; c) K.-L. Woon, C.-L. Yi, K.-C. Pan, M. K. Etherington, C.-C. Wu, K.-T. Wong, A. P. Monkman, *J. Phys. Chem. C* **2019**, *123*, 12400-12410; d) K. Li, Y. Zhu, B. Yao, Y. Chen, H. Deng, Q. Zhang, H. Zhan, Z. Xie, Y. Cheng, *Chem. Commun.* **2020**, *56*, 5957-5960; e) S.-Y. Yang, Q.-S. Tian, Y.-J. Yu, S.-N. Zou, H.-C. Li, A. Khan, Q.-H. Wu, Z.-Q. Jiang, L.-S. Liao, *J. Org. Chem.* **2020**, *85*, 10628-10637.

[6] a) S. Shao, J. Hu, X. Wang, L. Wang, X. Jing, F. Wang, *J. Am. Chem. Soc.* **2017**, *139*, 17739-17742; b) J. Hu, Q. Li, X. Wang, S. Shao, L. Wang, X. Jing, F. Wang, *Angew. Chem. Int. Ed.* **2019**, *58*, 8405-8409; *Angew. Chem.* **2019**, 131, 8493; c) C. M. Tonge, Z. M. Hudson, *J. Am. Chem. Soc.* **2019**, *141*, 13970-13976.

[7] X. Tang, L.-S. Cui, H.-C. Li, A. J. Gillett, F. Auras, Y.-K. Qu, C. Zhong, S. T. E. Jones, Z.-Q. Jiang, R. H. Friend, L.-S. Liao, *Nat. Mater.* **2020**. DOI: 10.1038/s41563-020-0710-z.

[8] Q. Li, J. Hu, J. Lv, X. Wang, S. Shao, L. Wang, X. Jing, F. Wang, *Angew. Chem. Int. Ed.*, **2020**, DOI: 10.1002/anie.202008912; *Angew. Chem. Int. Ed.*, **2020**, DOI: 10.1002/ange.202008912.

[9] Y. Wada, H. Nakagawa, S. Matsumoto, Y. Wakisaka, H. Kaji, *Nat. Photon.* **2020**, *14*, 643-649.

[10] a) J.-A. Lin, S.-W. Li, Z.-Y. Liu, D.-G. Chen, C.-Y. Huang, Y.-C. Wei, Y.-Y. Chen, Z.-H. Tsai, C.-Y. Lo, W.-Y. Hung, K.-T. Wong, P.-T. Chou, *Chem. Mater.* **2019**, *31*, 5981-5992; b) X.-K. Chen, B. W. Bakr, M. Auffray, Y. Tsuchiya, C. D. Sherrill, C. Adachi, J.-L. Bredas, *J. Phys. Chem. Lett.* **2019**, *10*, 3260-3268; c) X. Cai, Z. Qiao, M. Li, X. Wu, Y. He, X. Jiang, Y. Cao, S.-J. Su, *Angew. Chem. Int. Ed.* **2019**, *58*, 13522-13531; *Angew. Chem.* **2019**, *131*, 13656-13665.

[11] A. Wakamiya, H. Nishimura, T. Fukushima, F. Suzuki, A. Saeki, S. Seki, I. Osaka, T. Sasamori, M. Murata, Y. Murata, H. Kaji, *Angew. Chem. Int. Ed.* **2014**, *53*, 5800-5804; *Angew. Chem.* **2014**, *126*, 5910-5914.

[12] a) D. H. Ahn, S. W. Kim, H. Lee, I. J. Ko, D. Karthik, J. Y. Lee, J. H. Kwon, *Nat. Photon.* **2019**, *13*, 540-546; b) B. Adelizzi, P. Chidchob, N. Tanaka, B. A. G. Lamers, S. C. J. Meskers, S. Ogi, A. R. A. Palmans, S. Yamaguchi, E. W. Meijer, *J. Am. Chem. Soc.* **2020**, DOI: 10.1021/jacs.0c06921.

[13] L.-S. Cui, H. Nomura, Y. Geng, J. U. Kim, H. Nakanotani, C. Adachi, *Angew. Chem. Int. Ed.* **2017**, *56*, 1571-1575; *Angew. Chem.* **2017**, 129, 1593-1597.

[14] X.-L. Chen, J.-H. Jia, R. Yu, J.-Z. Liao, M.-X. Yang, C.-Z. Lu, *Angew. Chem. Int. Ed.* **2017**, *56*, 15006-15009; *Angew. Chem.* **2017**, 129, 15202-15205.

[15] L. Sun, W. Hua, Y. Liu, G. Tian, M. Chen, M. Chen, F. Yang, S. Wang, X. Zhang, Y. Luo, W. Hu, *Angew. Chem. Int. Ed.* **2019**, *58*, 11311-11316; *Angew. Chem.* **2019**, 131, 11433-11438.

[16] J. Huang, H. Nie, J. Zeng, Z. Zhuang, S. Gan, Y. Cai, J. Guo, S.-J. Su, Z. Zhao, B. Z. Tang, *Angew. Chem. Int. Ed.* **2017**, *56*, 12971-12976; *Angew. Chem.* **2017**, 129, 13151-13156.

Entry for the Table of Contents

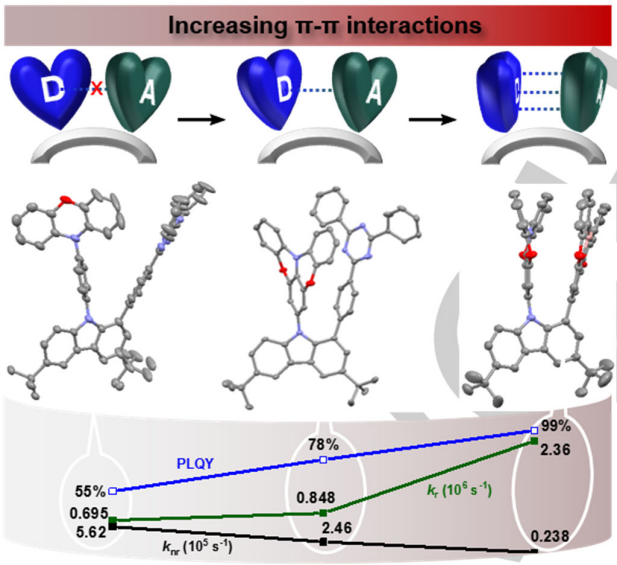

The orientation of donor and acceptor has been controlled for the development of thermally-activated delayed fluorescence emitters featuring intramolecular through-space charge transfer excited state. With maximized cofacial π-π interactions between the quasiplanar donor and acceptor segments, a substantial enhancement of radiative decay rate together with suppressed nonradiative decay was resulted to give an almost unity emission efficiency.